Cellular Signalling 63 (2019) 109366

Contents lists available at ScienceDirect

Cellular Signalling

journal homepage: www.elsevier.com/locate/cellsig

Arrestin-3 interaction with maternal embryonic leucine-zipper kinase

Nicole A. Perry[a,1], Kevin P. Fialkowski[a,2], Tamer S. Kaoud[b,c], Ali I. Kaya[a], Andrew L. Chen[b], Juliana M. Taliaferro[b], Vsevolod V. Gurevich[a], Kevin N. Dalby[b], T.M. Iverson[a,d,e,f,*]

[a] Department of Pharmacology, Vanderbilt University, Nashville, TN 37232-0146, USA
[b] Division of Chemical Biology & Medicinal Chemistry, The University of Texas at Austin, Austin, TX 78712, USA
[c] Medicinal Chemistry Department, Faculty of Pharmacy, Minia University, Minia 61519, Egypt
[d] Department of Biochemistry, Vanderbilt University, Nashville, TN 37232-0146, USA
[e] Center for Structural Biology, Vanderbilt University, Nashville, TN 37232-0146, USA
[f] Vanderbilt Institute of Chemical Biology, Vanderbilt University, Nashville, TN 37232-0146, USA

ARTICLE INFO

Keywords:
Maternal embryonic leucine-zipper kinase (MELK)
Arrestin
Cell fate signaling
Protein-protein interactions

ABSTRACT

Maternal embryonic leucine-zipper kinase (MELK) overexpression impacts survival and proliferation of multiple cancer types, most notably glioblastomas and breast cancer. This makes MELK an attractive molecular target for cancer therapy. Yet the molecular mechanisms underlying the involvement of MELK in tumorigenic processes are unknown. MELK participates in numerous protein-protein interactions that affect cell cycle, proliferation, apoptosis, and embryonic development. Here we used both *in vitro* and in-cell assays to identify a direct interaction between MELK and arrestin-3. A part of this interaction involves the MELK kinase domain, and we further show that the interaction between the MELK kinase domain and arrestin-3 decreases the number of cells in S-phase, as compared to cells expressing the MELK kinase domain alone. Thus, we describe a new mechanism of regulation of MELK function, which may contribute to the control of cell fate.

1. Introduction

Maternal embryonic leucine-zipper kinase (MELK) is a serine/threonine kinase of the AMPK/Snf1 family [1]. Unlike other family members, MELK does not require an upstream kinase activator and can self-activate *via* auto-phosphorylation *in vitro* [2]. MELK is highly conserved across species and is thought to play a role in cell cycle regulation, proliferation, and mitosis [1].

While the functions and regulatory mechanisms of MELK are just starting to be elucidated, MELK has been linked to several cell fate-related processes. For example, it has been demonstrated that in mice MELK induces phosphorylation and activation of apoptosis signal-regulating kinase 1 (ASK1), which activates cell death pathways [3]. In contrast, overexpression of MELK in breast cancer cell lines results in aggressive cell proliferation and suggests that the kinase may function as a driver oncogene [4,5]. These contradictory findings suggest that the role of MELK in pro- and anti-apoptotic pathways may be context-dependent.

Many signaling proteins have been identified as potential regulators of MELK activity. MELK has been proposed to increase transcription of oncogenes through interactions with transcription factors (FOXM1 [6,7], EIF4B [8], ZPR9 [9], and NIPP1 [9]), aid in DNA damage repair *via* regulation of p53 and ATM [7,10], and act as a cell cycle regulator [11]. MELK may also activate proteins that induce cell death, such as ASK1 [3] and Smads [12]. While these interacting partners and overexpression of MELK in various cancer types suggest the physiological importance of MELK, the molecular mechanisms underlying these interactions and their biological consequences remain unclear. More studies are needed to determine the exact role of MELK in disease progression and whether other regulators of its activity exist.

Here, we identify a novel interacting partner for MELK, arrestin-3.[3] While the arrestin proteins are best known for their role in the desensitization and internalization of G protein-coupled receptors (GPCRs) [13–16], they also interact with, and affect the activity of, other proteins, including Src family tyrosine kinases [17,18], mitogen-activated protein kinases and their upstream activators [19–23], and E3

* Corresponding author at: Department of Pharmacology, Vanderbilt University, Nashville, TN 37232, USA.
E-mail address: tina.iverson@vanderbilt.edu (T.M. Iverson).
[1] Present address: Department of Surgery, Columbia University in the City of New York, New York, NY 10032, USA.
[2] Present address: College of Medicine, University of Arkansas for Medical Sciences, Little Rock, AR 72205, USA.
[3] We use the systematic names of arrestins, which are based on the order of cloning: arrestin-1 (historic names S-antigen, 48 kDa protein, visual or rod arrestin), arrestin-2 (β-arrestin or β-arrestin1), arrestin-3 (β-arrestin2 or hTHY-ARRX), and arrestin-4 (cone or X-arrestin).

https://doi.org/10.1016/j.cellsig.2019.109366
Received 15 April 2019; Received in revised form 23 July 2019; Accepted 24 July 2019
Available online 25 July 2019
0898-6568/

ubiquitin ligases [24,25]. A key regulatory role of the arrestin proteins is their ability to act as scaffolds or adaptors for kinases and phosphatases [26]. Mechanistically, the arrestins likely both bring kinases or phosphatases and their substrates into proximity and orient these optimally to facilitate signaling [23,27,28]. Many of these kinases and phosphatases that interact with arrestin are implicated in cell-fate signaling [29], which suggests that the MELK/arrestin-3 interaction as a target for therapeutic development.

We used a combination of biophysical techniques and in-cell assays to show that arrestin-3 interacts with MELK and that the interaction with the MELK kinase domain is biologically relevant. Conceivably, this interaction influences the subcellular localization of MELK, which may explain how it affects cell fate signaling pathways.

2. Results

2.1. Pull-down assay of the MELK kinase domain with arrestin-$3^{1\text{-}393}$

Because arrestin scaffolding of mitogen activated protein kinases (MAPKs) depends upon interactions with the MAPK kinase domain [27,30,31], we reasoned that MELK could similarly interact *via* its kinase domain and used the isolated kinase domain of MELK (residues 1-326 out of 651 residues) for initial studies. We combined this with the T167E mutant (denoted MELK$^{1\text{-}326,T167E}$). MELK$^{1\text{-}326,T167E}$ is a well-characterized mimic of the constitutively phosphorylated state [32] that is expected to predominate in the cell as a result of MELK autophosphorylation [9]. This mutation likely results in MELK favoring the activated conformation that is biologically the most probable interactor with scaffolds; the phosphorylation of Thr^{167} and Ser^{171} is required for full activation [9]. This MELK$^{1\text{-}326,T167E}$ was used in two separate *in vitro* pull-down assays with truncated arrestin-3 (residues 1–393, denoted below as arrestin-$3^{1\text{-}393}$), which is an established model for both GPCR-dependent and GPCR-independent arrestin activation [19,22,23,27,33–35]. This C-terminal truncation of arrestin-3 shifts the equilibrium from a "basal" to an "active" conformation while preserving known kinase binding sites.

To test whether MELK directly interacts with arrestin-3, we used an *in vitro* pull-down assay with purified proteins. This assay is useful in the detection of high-affinity interactions [36]. We evaluated both human and mouse MELK$^{1\text{-}326,T167E}$ binding to arrestin-$3^{1\text{-}393}$ (Fig. 1A). Within the kinase domain of MELK, these homologs share 94% sequence identity. The MELK kinase domain of both species exhibited equally strong binding to arrestin-$3^{1\text{-}393}$ (Fig. 1A). Therefore, for subsequent experiments we used the human isoform of MELK$^{1\text{-}326,T167E}$.

Prior work that evaluated the interaction between arrestin and MAPKs revealed that the presence of ATP significantly increased the affinity and suggested that the arrestin-binding elements of kinases included regions that changed conformation upon ATP binding [27]. Therefore, we tested whether the presence of physiological concentrations of ATP and $MgCl_2$ affected the binding of human MELK$^{1\text{-}326,T167E}$ to arrestin-$3^{1\text{-}393}$. In the presence of ATP and $MgCl_2$ the MELK$^{1\text{-}326,T167E}$ interaction with arrestin-$3^{1\text{-}393}$ was unchanged (Fig. 1B). Thus, the effect of ATP on the conformation of the kinase domain does not affect its interaction with arrestin-$3^{1\text{-}393}$. Because the ATP-binding pocket is located between the N- and C-lobes of the MELK kinase domain, and ATP likely affects the conformation of this interdomain region, we conclude that arrestin does not bind between the two kinase lobes [32].

2.2. Affinity of MELK$^{1\text{-}326,T167E}$ for arrestin-$3^{1\text{-}393}$

MicroScale Thermophoresis (MST) quantifies biomolecular interactions using the directed movement of molecules along a temperature gradient [37]. To measure the affinity of the kinase domain of human MELK$^{1\text{-}326,T167E}$ for arrestin-$3^{1\text{-}393}$, we used increasing concentrations of arrestin-$3^{1\text{-}393}$ (0–40 μM) in the presence of fluorescently-tagged MELK$^{1\text{-}326,T167E}$ (50 nM) and physiological concentrations of ATP and $MgCl_2$. In this assay, MELK$^{1\text{-}326,T167E}$ exhibited high affinity for arrestin-$3^{1\text{-}393}$ with a K_d of 130 ± 35 nM (Fig. 2). This interaction is likely biologically relevant, as MELK$^{1\text{-}326,T167E}$ binding to arrestin-3 is much tighter than observed in a highly-validated set of interactions between arrestin and members of the JNK3 cascade (~1–20 μM) [27].

2.3. Mapping the arrestin-3 binding site for MELK$^{1\text{-}326,T167E}$

Defining the interaction interfaces between proteins is crucial both for understanding the mechanism of binding and for targeted manipulation of signaling pathways. Protein-protein interactions are studied by a wide variety of techniques and can be probed using full-length

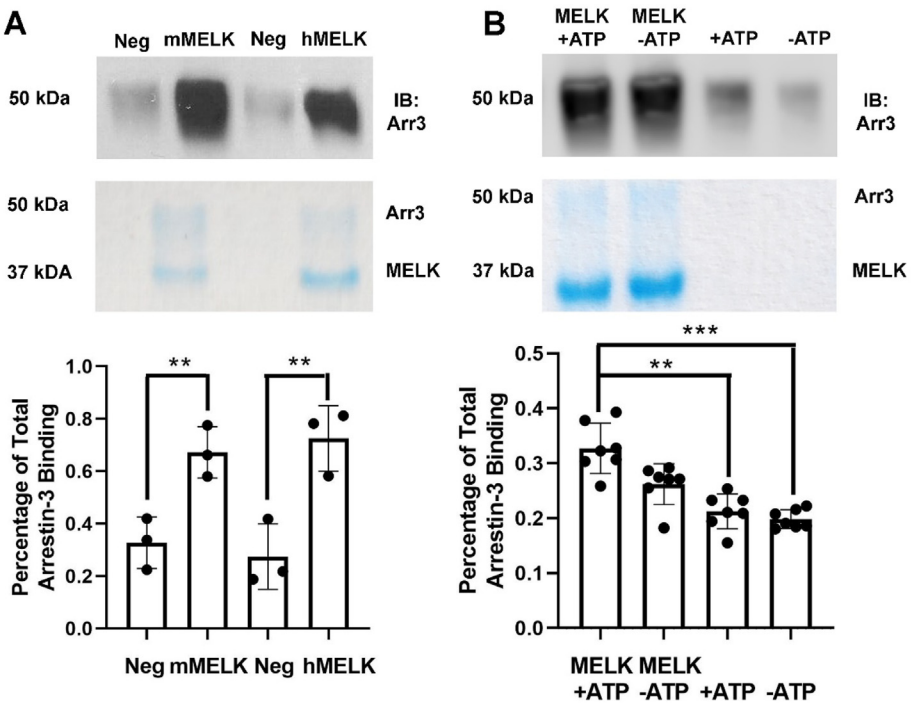

Fig. 1. Pull-down of purified MELK$^{1\text{-}326,T167E}$ with purified arrestin-$3^{1\text{-}393}$. (A) Analysis of mouse MELK$^{1\text{-}326,T167E}$ (10 μg; mMELK) and human MELK$^{1\text{-}326,T167E}$ (10 μg; hMELK) binding to bovine arrestin-$3^{1\text{-}393}$ (10 μg). Top: Representative Western blot of the eluates using a polyclonal anti-arrestin antibody (1:10,000, F431 [55]). Middle: Representative Coomassie staining of the eluates. Bottom: Quantification of arrestin-3 binding using densitometry. Intensity was compared to the negative control (beads alone) and binding is shown as a percentage of total arrestin-3 applied (n = 3). Statistical analysis was performed using Student's *t*-test (**, $p < .01$). (B) Analysis of human MELK$^{1\text{-}326,T167E}$ (10 μg) binding to bovine arrestin-$3^{1\text{-}393}$ (10 μg) in the absence or presence of 2 mM ATP and 4 mM $MgCl_2$. Top: Representative Western blot of the eluates using an anti-arrestin-3 antibody (1:10,000, F431). Middle: Representative Coomassie staining of the eluates. Bottom: Quantification of arrestin-3 binding using densitometry. Intensity was compared to the negative control (beads alone) and binding is displayed as a percentage of total arrestin-3 applied (n = 7). Statistical analysis was performed using Kruskal-Wallis test with multiple comparisons (**, $p < .01$; ***, $p < .001$).

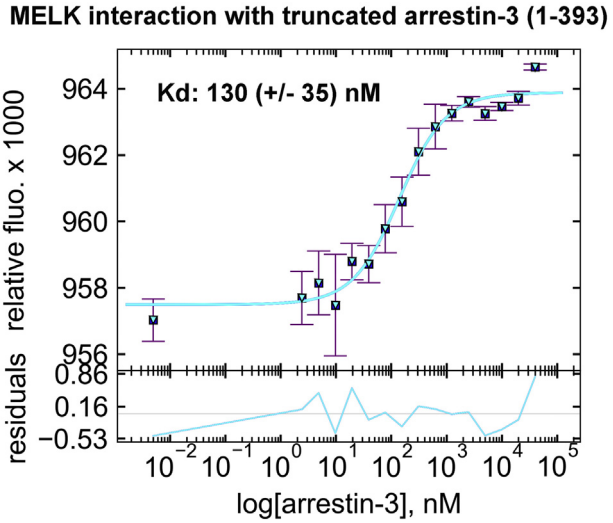

Fig. 2. The affinity of MELK$^{1\text{-}326,T167E}$ for arrestin-3$^{1\text{-}393}$ in the presence of ATP. A binding curve for bovine arrestin-3$^{1\text{-}393}$ with human MELK$^{1\text{-}326,T167E}$ in the presence of 1 mM ATP and 2 mM $MgCl_2$ is shown with the average K_d value (n = 3). Microscale thermophoresis was performed at a constant concentration of Tris-NTA-labeled His-MELK$^{1\text{-}326,T167E}$ (50 nM) with a serial dilution of arrestin-3$^{1\text{-}393}$ (0–40 μM). The binding isotherm was calculated using preset T-jump in the software PALMIST [56,57], and the graph was created in the program GUSSI.

proteins, separated protein domains, or peptides. Two distinct advantages of using peptides to study protein-protein interactions are the ease of synthesis and the ability to identify specific interaction sites [38]. Peptide arrays allow the identification of specific binding residue (s) within a complex interaction surface [39].

To identify the regions of arrestin-3 that are important for the interaction with MELK$^{1\text{-}326,T167E}$, we performed a 15-mer peptide scan of full-length arrestin-3 using 1 amino acid shifts (Fig. 3A, Supplementary Table 1). We classified peptides by the strength of their binding to MELK and mapped interaction regions onto the crystal structure of arrestin-3$^{1\text{-}393}$ (PDB entry 3P2D) [40] (Fig. 3B). Most of the interacting peptides were localized on the non-receptor-binding surface in folded arrestin-3$^{1\text{-}393}$, suggesting that GPCR-bound arrestin-3 can interact with MELK. Several peptides appear to be critical for the interaction. The first set of peptides encompasses residues A87-L109, previously termed T2A [35]. This region includes the α-helix of arrestin involved in the three-element interaction, which is part of the phosphate sensor [40]. The second group of peptides corresponds to arrestin residues T187-S203, Y209-T226 (previously T4 [35]), and V272-D291; these peptides encompass several β-strands on the non-receptor-binding surface of the C-domain (Fig. 3C, D). Third, a group of peptides corresponding to residues V165-Q173 also displayed strong binding. However, surface inaccessibility in the context of folded arrestin [33,38,40] suggests that these may be false positives. Indeed, this region is fairly hydrophobic, which could result in non-specific binding of these peptides to MELK. Collectively, these results suggest that MELK$^{1\text{-}326,T167E}$ binds elements in both arrestin domains, so that the observed high affinity interaction likely involves multiple sites (Fig. 2). This is similar to our previous finding that each kinase in the ASK1-MKK4/7-JNK3 and cRaf-MEK1-ERK1/2 cascades [41], as well as E3 ubiquitin ligase parkin [24] engage both arrestin domains.

2.4. Mapping the MELK site for arrestin-3$^{1\text{-}393}$ binding

To characterize the arrestin-3 binding site on MELK, we used a peptide array corresponding to full-length MELK (residues 1–651) using 3 amino acid shifts (Fig. 4A, Supplementary Table 2). This strategy revealed several regions of MELK that could be responsible for the interaction in the context of the folded protein (Fig. 4B). The highest binding was detected for residues N562-L582 in the KA-1 domain. It has been suggested that this domain must be disrupted to prevent autoinhibition of the kinase and maintain its activity [42,43]. The KA-1 domain was also implicated in membrane localization of MELK [43]. In addition, a second region of strong binding involved residues Y88-E108 of the kinase domain. Binding was also detected across several residues in the kinase (Fig. 4C, D). Of note, no interaction with arrestin-3$^{1\text{-}393}$ was detected in the activation segment of MELK (residues D150-E178), which is a region of the kinase that is important for activity [44]. Because an interaction with the activation segment might be anticipated to block kinase activity, this suggests that the kinase can retain biological function in complex with arrestin.

Mapping of these peptides is somewhat limited because only the isolated kinase domain of MELK has been crystallized (PDB 4IXP [42,45–48]), so it is not known whether residues N562-L582 of the KA-1 domain and Y88-E108 of the kinase domain form a contiguous surface in full-length MELK. Mapping Y88-E108 and other peptides with more moderate signal onto the crystal structure of the MELK kinase domain (PDB 4IXP, [42]) identifies that these peptides localize to the C-lobe (highlighted in red in Fig. 4B).

2.5. Mutational analysis of arrestin-3- and MELK-derived peptides pinpoints key interacting residues

To test whether the high-interaction peptides identified by array analysis contribute to the binding between arrestin-3 and MELK, we performed additional peptide array experiments using alanine scanning, charge reversal, and alanine substitution (Supplementary Figs. 1 and 2). First, we measured MELK$^{1–326,\ T167E}$ binding to the wild type (WT) and mutant T2A peptides (Supplementary Fig. 1). We found that most mutations weakened the MELK interaction compared to the control T2A peptide; however, a single charge reversal from lysine to glutamate at the twenty-second amino acid greatly enhanced the interaction (Supplementary Fig. 3A). To test MELK-derived peptides for binding with arrestin-3, we chose peptides from the kinase domain (YCPGGELFDYIISQDRLS) and the KA-1 domain (NVTTTRLVNPDQLLNEIMSIL), which demonstrated high binding in the initial screen (Supplementary Fig. 2). Again, most mutations weakened the arrestin-3$^{1\text{-}393}$ interaction compared to the control peptides (Supplementary Figs. 3B, C).

2.6. Arrestin-3$^{1\text{-}393}$ coimmunoprecipitates with full-length MELK and MELK$^{1\text{-}340}$ in cells

To validate our *in vitro* findings in a more biological context we assessed the MELK/arrestin-3$^{1\text{-}393}$ interaction in living cells using overexpression. This overexpression in HEK293 cells resulted in a 4.6-fold increase in arrestin-3 as compared to the endogenous levels of arrestin-3 in the same cell line (Supplementary Fig. 4). It should be noted that arrestin has uneven subcellular distribution and the effect of overexpression on this distribution is unknown. The MELK constructs used in these experiments did not carry the T167E mutation and could therefore be in an inactive or active state, depending on whether or not they were phosphorylated. We first used coimmunoprecipitation to test the ability of full-length MELK and arrestin-3$^{1\text{-}393}$ to interact (Fig. 5). We observed a robust binding of arrestin-3$^{1\text{-}393}$ with full-length MELK, suggesting that the interaction is likely biologically relevant.

To assess whether the separated kinase domain binds arrestin-3$^{1\text{-}393}$ in cells, we repeated our assay using several DNA ratios with a truncated MELK construct, MELK$^{1\text{-}340}$ (Fig. 6). We detected a modest binding of arrestin-3$^{1\text{-}393}$ and MELK$^{1\text{-}340}$ at a 1:1 DNA transfection ratio; however, it was not as strong as that observed for the full-length protein. This suggests that regions of MELK outside of the kinase domain also interact with arrestin, a conclusion consistent with the *in vitro* peptide array data (Fig. 4).

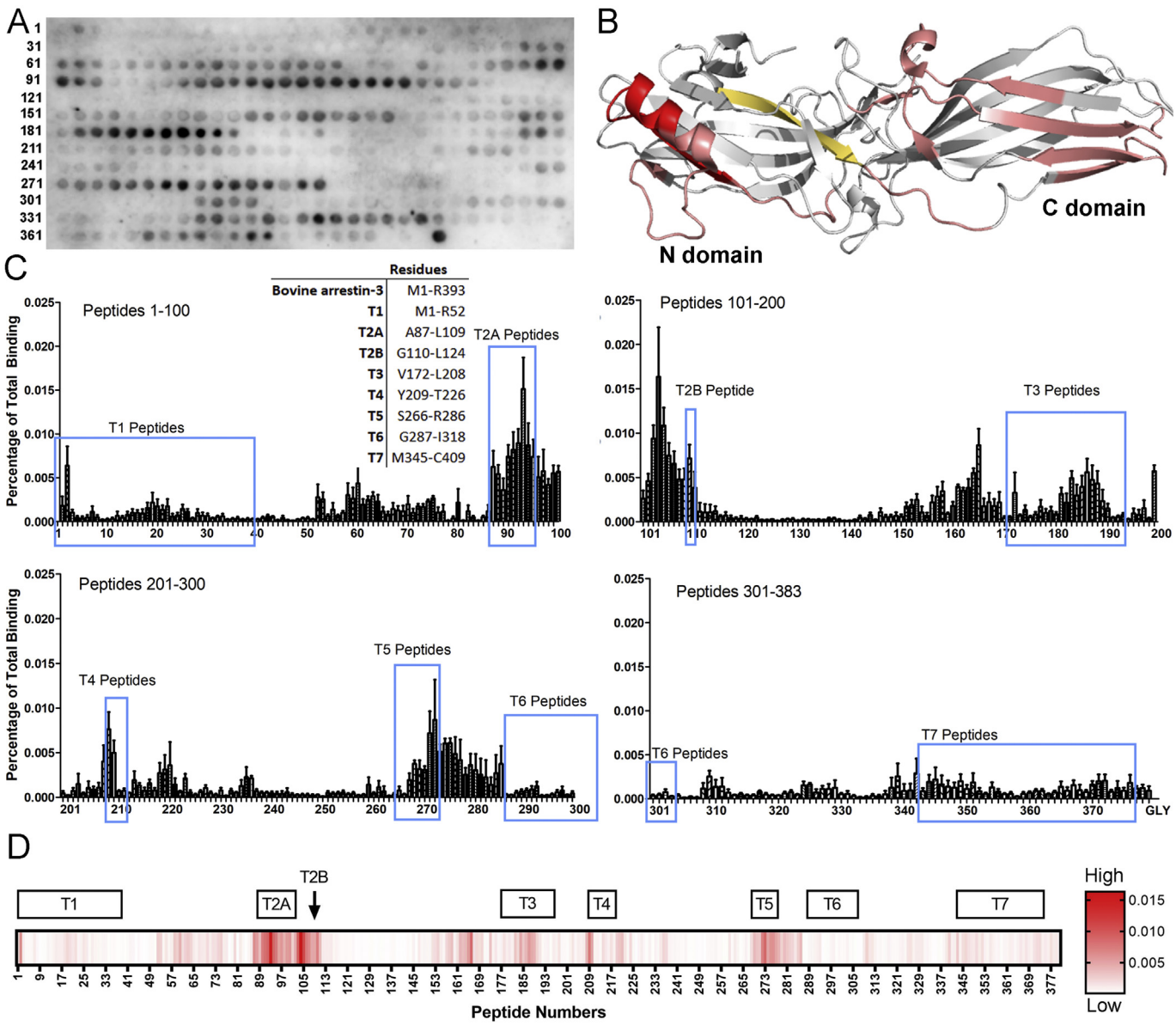

Fig. 3. MELK$^{1\text{-}326,T167E}$ binding sites on arrestin-3. (A) Representative peptide blot (15-mer) of bovine arrestin-3-derived peptides (residues 1–393, 1 amino acid shifts). (B) Map of interaction sites for MELK$^{1\text{-}326,T167E}$ on arrestin-3 (PDB 3P2D [34]). Peptides calculated to be in the top 1% for binding to MELK$^{1\text{-}326,T167E}$ are highlighted in red and top 10% in salmon. The peptide V165-Q173 (shown in orange-yellow) demonstrated binding within the top 10% but is likely a false positive due to its surface inaccessibility in both basal [34] and active [35] arrestin-3 structures. (C) Quantified binding of MELK$^{1\text{-}326,T167E}$ to arrestin-3-derived peptides. Binding was measured as a percentage of total intensity on the membrane. A 15-mer glycine peptide was used to determine non-specific interactions. Inset: Peptide segments corresponding to the non-receptor surface of arrestin-3. The corresponding regions are circled in blue on the quantification. (D) Heat map using a single gradient to display ranges of binding was calculated using GraphPad Prism 8.0.2. Peptides corresponding to the non-receptor-binding surface of arrestin-3 are shown above. (For interpretation of the references to color in this figure legend, the reader is referred to the web version of this article.)

2.7. The number of S-phase cells is decreased by co-expression of arrestin-3$^{1\text{-}393}$ with MELK$^{1\text{-}340}$

Over-expression of MELK has been demonstrated in several cancer types and is often correlated with poor prognosis [4]. As our *in vitro* and in-cell studies support an interaction between the MELK kinase domain and arrestin-3, we chose to measure the effect of arrestin-3$^{1\text{-}393}$, a MELK fragment containing the kinase and UBA domain (MELK$^{1\text{-}340}$; residues 1–340), and arrestin-3$^{1\text{-}393}$/MELK$^{1\text{-}340}$ on the cellular transition to S-phase. To this effect, we directly measured DNA synthesis using 5-ethynyl-2′-deoxyuridine (EdU) incorporation as a readout. EdU is a nucleoside analog of thymidine that is readily incorporated into replicating DNA and can be detected using fluorescent azides [49]. HEK293 arrestin-2/3 knockout cells [50] were incubated in media with or without EdU following transfection. Cells were then fixed and incubated with Alexa Flour 488 picolyl azide, whereupon flow cytometry was used to determine the percentage of S-phase cells in the population (Fig. 7). Untransfected cells with EdU treatment were used as a negative control for gating purposes (gray trace in Fig. 7A, gating schematic shown in Fig. 7B) and yielded 22 ± 10% S-phase cells. Three replicates yielded the following percentages of S-phase cells: 17 ± 5% for arrestin-3$^{1\text{-}393}$ transfection, 37 ± 6% for MELK$^{1\text{-}340}$ transfection, and 15 ± 6% for cells expressing both proteins. Thus arrestin-3$^{1\text{-}393}$ significantly reduced the observed increase in S-phase cells associated with MELK$^{1\text{-}340}$ expression. Conceivably, arrestin-3, which directly binds ASK1 [19,22,41,51], facilitates MELK-dependent ASK1 activation, which would suppress proliferation.

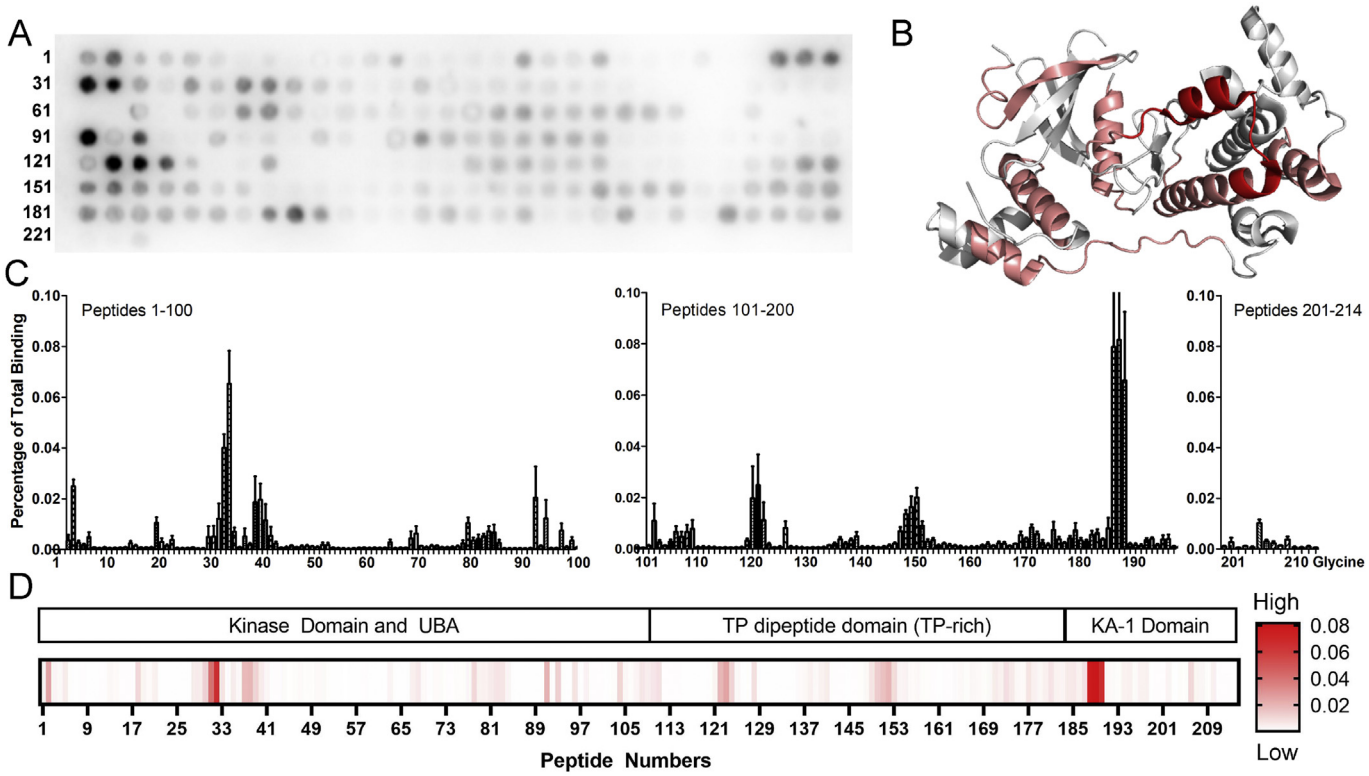

Fig. 4. Arrestin-3$^{1\text{-}393}$ binding sites on MELK$^{1\text{-}651}$. (A) Representative peptide blot using 15-mers derived from human MELK (residues 1–651, 3 amino acid shifts). (B) Map of interaction sites for arrestin-3$^{1\text{-}393}$ on MELK (PDB 4BL1; to be published [37]). Peptides were analyzed using conditional formatting and those that exhibited binding to arrestin-3$^{1\text{-}393}$ within the top 10% are highlighted in salmon, while those binding within the top 5% are shown in red. Only 347 residues are visible in the crystal structure (up to peptide 107 in the array). Therefore, the peptides with the greatest binding (188-190; sequence NVTTTRLVNPDQLLNEIMSIL from the C-terminal KA1 domain), cannot be displayed. (C) Quantified binding of arrestin-3$^{1\text{-}393}$ to MELK-derived peptides. Arrestin-3$^{1\text{-}393}$ binding was measured as a percentage of total intensity of all spots. (D) Heat map using a single gradient to display ranges of binding was calculated using GraphPad Prism 8.0.2. Corresponding MELK domains are shown above. (For interpretation of the references to color in this figure legend, the reader is referred to the web version of this article.)

3. Discussion

Previous proteomic analysis of the non-visual arrestins activated by the angiotensin 1 receptor showed > 100 effectors that bind arrestins either directly or indirectly [26]. This list, however, did not include MELK as a potential binding partner. In contrast, our data indicate a direct (Fig. 1), high affinity (Fig. 2) interaction between the MELK kinase domain (MELK$^{1\text{-}326,T167E}$) and arrestin-3$^{1\text{-}393}$. This observed difference could be due to the limitations of the methods, or the differences in protein constructs used. For example, the proteomics study used the angiotensin II type 1a receptor to measure proteins bound to arrestin after agonist stimulation; the detected molecules are expected to be biased toward the effectors activated by this receptor.

Consideration of how this protein-protein interaction might affect MELK activity draws from known roles of arrestin. Arrestins can act as adaptors or scaffold proteins with multiple biological roles. For example, arrestin scaffolds are commonly thought to regulate signaling of cytoplasmic proteins, a process that includes both kinase activation and signal amplification [26]. In considering this role within the context of the data presented here, multiple studies have demonstrated that MELK undergoes autophosphorylation [9,45], and our data show that the phosphomimetic variant of MELK binds robustly to arrestin-3 (Fig. 2). Moreover, the interaction with arrestin-3 appears to influence the biological function of the active MELK kinase domain, by pushing toward anti-proliferative, rather than proliferation pathways (Fig. 7). Together, this suggests that the arrestin-3-MELK interaction is not involved in the initial phosphorylation and activation of MELK.

A second proposed role for arrestins is to control the subcellular localization of bound effectors, as is demonstrated for MAPK cascades [22,23,30,41,52]; [53], and ubiquitin ligase Mdm2 [53,54]. One possibility is that arrestin localizes MELK to a specific region in the cell in order to direct MELK activity to particular substrates. MELK exhibits cell-cycle dependent localization and has been shown to associate with the scaffold protein anillin along with other proteins involved in cytokinesis [55]. The KA-1 domain of MELK has also been shown to regulate MELK association with cellular membranes [9,43,56]. This could explain the prior controversial findings that the cellular effects of MELK activity are context dependent [3–5]. Given the role of MELK activity in controlling the cell cycle, understanding how the arrestin-3/MELK interaction influences MELK function could provide a new avenue for modulating MELK activity.

It should be emphasized that we observe *in vitro* binding between arrestin-3$^{1\text{-}393}$ and MELK$^{1\text{-}326,T167E}$ (Fig. 1), which corresponds to the kinase domain of MELK. Although our peptide array data (Fig. 4) and pull downs from cells (compare Fig. 5 and Fig. 6) suggest that the interaction between arrestin and MELK involves both the kinase domain and other regions outside of this domain, most notably the TP dipeptide-rich domain and the KA-1 domain, the interaction between arrestin-3 and the MELK kinase domain appears to be sufficient to alter cell fate (Fig. 7). In addition to regulating membrane association, the KA-1 domain has been implicated in autoinhibition of MELK through an interaction with the UBA region [9,43,56]. While the hypotheses regarding possible binding mechanisms are limited by the absence of a structure of full-length MELK, it is tempting to speculate that arrestin-3$^{1\text{-}393}$ binding to the KA-1 domain prevents MELK autoinhibition and promotes kinase activity. If this activity is directed toward ASK1, an established arrestin-3 partner, this would explain arrestin-3-dependent reduction in S-phase cells (Fig. 7). Further experimentation is necessary to test this hypothesis.

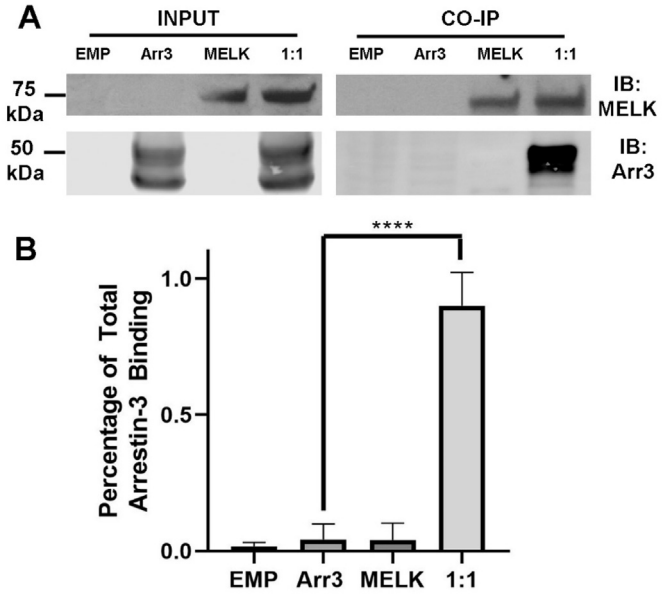

Fig. 5. Co-immunoprecipitation of wild-type MELK$^{1\text{-}651}$ with arrestin-3$^{1\text{-}393}$. (A) Western analysis of coimmunoprecipitation. HEK293 arrestin-2/3 knockout cells were transfected with empty vector (20 μg), HA-arrestin-3$^{1\text{-}393}$ (10 μg), FLAG-MELK$^{1\text{-}651}$ (10 μg), or both plasmids encoding arrestin-3 and MELK at a 1:1 DNA ratio for 48 h prior to immunoprecipitation with FLAG primary antibody. Western analysis was performed using anti-arrestin (1:10,000; F431) and anti-FLAG (1: 1,000; F3165 Sigma) antibodies. (B) Arrestin-3$^{1\text{-}393}$ co-immunoprecipitation with MELK$^{1\text{-}651}$ was quantified using densitometric analysis of arrestin-3 blots. Empty vector and non-specific arrestin-3 binding (no bait control) are also shown. Statistical analysis was performed using One-way ANOVA followed by Dunnett's *post hoc* test with correction for multiple comparisons (****, $p < .0001$).

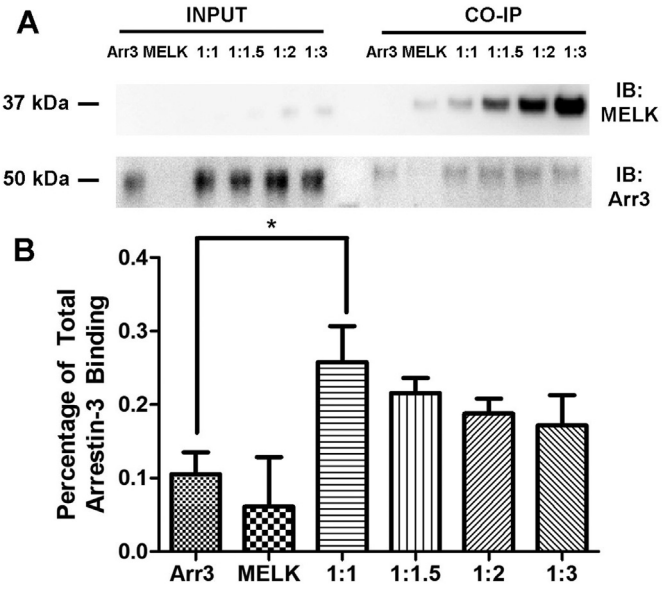

Fig. 6. Co-immunoprecipitation of wild-type MELK$^{1\text{-}340}$ with arrestin-3$^{1\text{-}393}$. (A) Western analysis of coimmunoprecipitation. HEK293 arrestin-2/3 knockout cells were transfected with HA-arrestin-3$^{1\text{-}393}$ (1 μg), FLAG-MELK$^{1\text{-}340}$ (1 μg), or both plasmids encoding arrestin-3 and MELK at indicated DNA ratios for 48 h prior to immunoprecipitation with FLAG primary antibody. Western analysis was performed using anti-arrestin (1:10,000; F431) and anti-FLAG (1: 1,000; F3165 Sigma) antibodies. (B) Arrestin-3$^{1\text{-}393}$ co-immunoprecipitation with MELK$^{1\text{-}340}$ was quantified using densitometric analysis of arrestin-3 blots. Non-specific arrestin-3 binding (no bait control) is also shown. Statistical analysis was performed using One-way ANOVA followed by Tukey's *post hoc* test with correction for multiple comparisons (*, $p < .05$).

4. Experimental procedures

4.1. Purified proteins

For this study, we used a fragment of MELK including its kinase domain and the flanking ubiquitin-associated domain (residues 1–326). This fragment retains full catalytic activity [9] and is easier to purify than full-length MELK. The MELK construct used also contained a T167E mutation (denoted MELK$^{1\text{-}326,T167E}$), a well-characterized mimic of the constitutively phosphorylated state [32] mimicking its activation (phosphorylation at Thr^{167} and Ser^{171} is required for full activation). The phosphorylated kinase is expected to predominate in the cell as a result of MELK autophosphorylation [9].

We used a truncated arrestin-3 (residues 1–393, denoted below as arrestin-3$^{1\text{-}393}$) construct for all analyses. This truncated version of arrestin-3 is an established model for both GPCR-dependent and GPCR-independent arrestin activation [19,22,23,27,33–35] as the C-terminal deletions in arrestin shift the equilibrium from a "basal" to an "active" conformation. This construct eliminates the need for arrestin activation *via* GPCRs and allows arrestin-3 to sample multiple active conformations.

Arrestin-3$^{1\text{-}393}$ was purified as previously described [57,58]. For MELK expression, a BL21 DE3 pLysS glycerol stock of MELK T167E (residues 1–326) in pET21b was used to inoculate a 120 mL starter culture overnight at 30 °C, 205 rpm. Each 1 L was inoculated using 10 mL of overnight culture. Expression was induced with 500 μM IPTG after cells reached an OD_{600} 0.6, and the temperature was reduced to 17 °C for ~18 h. The cells were pelleted by centrifugation at 6000 ×*g*, 10 min. The pellets were subjected to one cycle of freeze-thaw before adding the lysis buffer (20 mM Tris-HCl pH 7.5, 300 mM NaCl, 50 mM imidazole, 25 μL DNAse, 500 μL Pepstatin A, 100 μL leupeptin, 2 mM TCEP). The crude lysate was sonicated for 4 min (5 s on, 10 s off, 75% amplitude (FB505 Sonic Dismembrator, Fisher Scientific) before pelleting debris at 18,000 ×*g* for 30 min).

The clarified lysate was loaded onto a HisTrap column (GE) at 2.5 mL/min in wash buffer (20 mM Tris-HCl pH 7.5, 300 mM NaCl, 50 mM imidazole). Bound protein was eluted with a 0–200 mM imidazole gradient in elution buffer (20 mM Tris-HCl pH 7.5, 300 mM NaCl). The fractions were analyzed by SDS-PAGE. Pooled fractions containing MELK$^{1\text{-}326}$ were concentrated and subjected to size exclusion chromatography on a Superdex S200 Increase 10/300 GL column equilibrated with 25 mM HEPES pH 7.3, 300 mM NaCl, and 2 mM TCEP.

4.2. In vitro pull-down assay

Ni-NTA agarose resin (Qiagen) was rinsed three times with wash buffer (20 mM Tris-HCl pH 7.5, 150 mM NaCl, 10 mM imidazole pH 7.5, 0.1 mg/mL BSA) and 25 μL of the 50% slurry was aliquoted into each tube. His- MELK$^{1\text{-}326,T167E}$ (10 μg in 25 μL wash buffer) was immobilized on agarose resin for 1 h at 4 °C with gentle rotation. Arrestin-3$^{1\text{-}393}$ (10 μg in 50 μL wash buffer) was added to the suspension and incubated with slow rotation for 2 h at 4 °C in the presence or absence of 2 mM ATP and 4 mM $MgCl_2$. Samples were transferred to centrifuge filters (Durapore® PVDF-0.65 μm) and washed quickly with 900 μL 50 mM HEPES pH 7.3 and 150 mM NaCl. Proteins were eluted with 100 μL 50 mM HEPES pH 7.3, 150 mM NaCl, and 100 mM imidazole. The eluates were immediately precipitated with methanol (90% final concentration), air dried, and dissolved in SDS sample buffer (40 μL Laemmli 2×). The samples were analyzed using SDS-PAGE and Western blotting, as described [35].

4.3. Microscale thermophoresis

MST experiments were performed using the Monolith NT.115 instrument (NanoTemper Technologies GmbH). The Monolith™ His-Tag

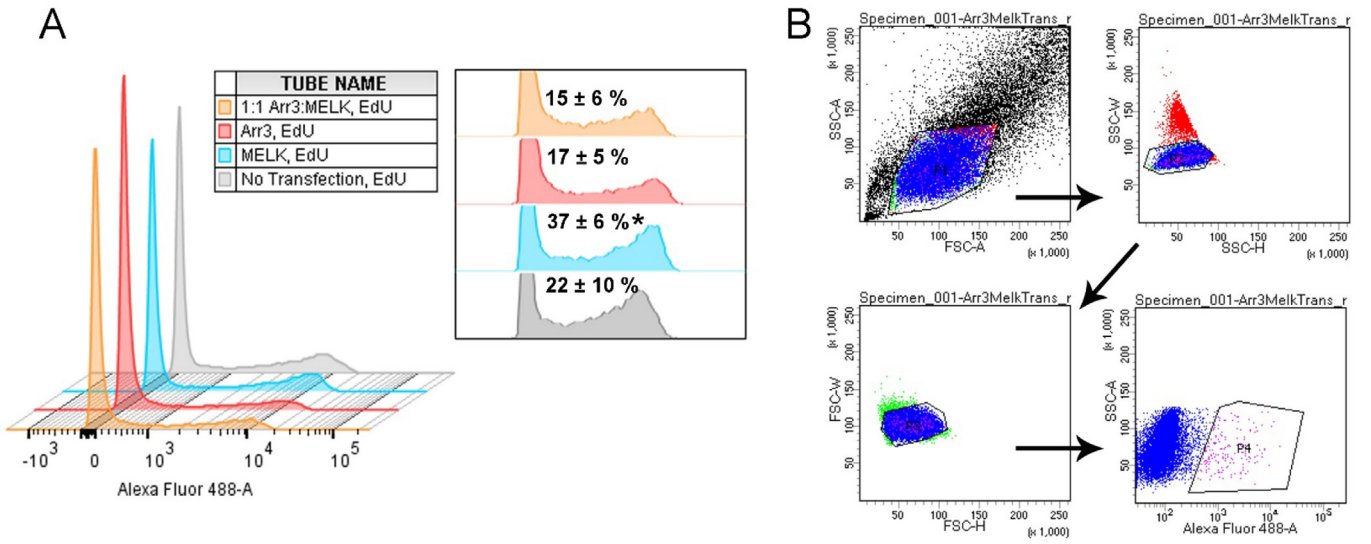

Fig. 7. The effect of wild-type MELK$^{1\text{-}340}$ and arrestin-3$^{1\text{-}393}$ expression on the fraction of cells in S-phase. HEK293 arrestin-2/3 knockout cells were transfected with HA-arrestin-3$^{1\text{-}393}$ (1 μg) (red), FLAG-MELK$^{1\text{-}340}$ (1 μg) (blue), or a fixed DNA ratio of plasmids encoding the two proteins (1 μg:1 μg) (orange), and the number of cells in S-phase was measured using the Click-iT™ EdU Alexa Fluor 488 Imaging Kit (ThermoFisher Scientific), followed by flow cytometry. (A) A representative histogram shows data from cells labeled with Alexa Fluor 488 picolyl azide analyzed using a 3-laser LSRII (BD Biosciences). The inset shows the relative heights of the second distribution (Alexa Fluor 488 positive cells) with the percentages of cells in S-phase for combined experiments (n = 3). Analysis was completed on FlowJo 10.1.5 (FlowJo LLC). Statistical analysis was performed using One-way ANOVA followed by Tukey's post-hoc test (*, $p < .05$ to 1:1 Arr3:MELK). The first distribution represents cells that are not proliferating, while the second distribution represents cells in S-phase. (B) The gating strategy used for histogram generation. Cells were initially sorted by scatter (SSC-A by FSC-A) (P1) to determine the population of living cells, then by single cells (SSC-W by SSC-H) (P2), then singlets (FSC-W by FSC-H) (P3), and finally by cells positive for Alexa Fluor 488 (SSC-A by Alexa Fluor 488) (P4). (For interpretation of the references to color in this figure legend, the reader is referred to the web version of this article.)

Labeling Kit RED-tris-NTA was used to label human His-MELK$^{1\text{-}326,T167E}$ following the manufacturer's protocol (100 nM final concentration of His-MELK$^{1\text{-}326,T167E}$ in PBS-T buffer). Purified arrestin-3$^{1\text{-}393}$ was diluted to a starting concentration of 80 μM in MST buffer (20 mM MOPS pH 7.5, 150 mM NaCl, 2 mM TCEP, 0.05% Tween-20). A 16-step dilution series was prepared by aliquoting 10 μL of MST buffer to 15 tubes. A 20 μL aliquot of the prepared arrestin-3$^{1\text{-}393}$ sample was placed in the first tube, and 10 μL was transferred to the second tube and mixed well by pipetting (1,1 dilution series). The final tube did not contain any arrestin-3$^{1\text{-}393}$ and served as a blank. To all tubes, 10 μL of labeled His-MELK$^{1\text{-}326,T167E}$ in the presence of 1 mM ATP and 2 mM $MgCl_2$ was added. After 15–30 min incubation on ice, the samples were transferred to Standard Monolith NT™ Capillaries. Each capillary was scanned using the MST instrument (40% LED, 40% MST power) and data were analyzed using PALMIST [59,60]. Measured fluorescence was normalized and averaged, and the data were fit using a 1:1 binding model. The preset T-jump was used to calculate binding isotherms. All data were displayed using GUSSI.

4.4. Peptide array synthesis

The ResPep SL peptide synthesizer was used with standardized SPOT synthesis protocols using 15-residue peptides, as previously described [61]. A 15-mer glycine peptide was used as a negative control in all experiments. Peptide assembly was conducted on solid support by the ResPep SL *via* a peptide amide linker using Fmoc-chemistry. The sequences were derived from either the full-length bovine arrestin-3 or full-length human MELK. After peptide synthesis, the amino protecting group was removed using piperidine (20% (v/v) solution in dimethylformamide) and extensive washing. The membranes were immersed for 1 h in a solution of 95% trifluoroacetic acid (TFA) and 3% triisopropylsilane with slight agitation. After the TFA solution was removed, the membranes were washed in dichloromethane four times 10 min each, after which they were washed in dimethylformamide four times 10 min each, and finally washed in ethanol two times 2 min each. The membranes were dried under the hood and stored at 4 °C.

4.5. Peptide membrane blots

Dried membranes were activated by soaking in 100% ethanol for 5 min at room temperature and rehydrated by rinsing two times 5 min in water. The membranes were then blocked in a 20 mL solution of 5% non-fat dry milk in Tris-buffered saline with 0.1% Tween-20 (TBS-T) for 1 h. Then, the membranes were washed three times 5 min each in TBS-T before overnight incubation with prey protein (0.2 μM MELK$^{1\text{-}326,T167E}$ or 0.3 μM arrestin-3$^{1\text{-}393}$) in binding buffer (MELK: 20 mM Tris-HCl, pH 7.5, 300 mM NaCl, 5 mM DTT; arrestin-3: 20 mM MOPS pH 7.5, 150 mM NaCl, 2 mM TCEP). The following day the membranes were washed three times for 5 min each in TBS-T at room temperature and then incubated with primary antibody (1:1000 Aviva anti-MELK or 1:5000 anti-arrestin rabbit polyclonal antibody F431 [58]) for 1 h at room temperature. The membranes were then washed three times, 5 min each, in TBS-T, incubated for 1 h with the corresponding HRP-conjugated secondary antibody (1: 4000 dilution; Abcam) in TBS-T, and washed three times 5 min each in TBS-T. The membranes were developed using a peroxide solution (SuperSignal West Pico) and visualized using a Bio-Rad Gel Doc Imager. Individual dots were analyzed by densitometry using a protein array analyzer (ImageJ). Individual dot density was expressed as a percentage of total binding across the entire membrane. Peptides were mapped onto either the arrestin-3 structure (PDB 3P2D [40]) or MELK structure (PDB 4BL1; to be published [45]) using conditional formatting in Excel (color scales) to identify the highest and lowest intensity values in relation to one another.

4.6. Co-immunoprecipitation of arrestin-3$^{1\text{-}393}$ with full-length MELK or MELK$^{1\text{-}340}$

HEK293 arrestin-2/3 knockout cells [50,62] were transfected with HA-arrestin-3 (10/1 μg), FLAG-MELK/FLAG-MELK-340-WT (10/1 μg), or a fixed ratio of the two plasmids for 48 h. Cells were washed in

phosphate-buffered saline (PBS) before incubation with RIPA buffer (Sigma) for 1 h. Lysed cells were centrifuged for 10 min at maximum speed (10,000 ×*g*) at 4 °C and the supernatant was precleared by 50 μL of suspension of Protein G Sepharose (supplied as aqueous ethanol suspension; Sigma; washed with PBS) for 1 h. Samples were then centrifuged at low speed (3200 ×*g*) to remove the beads, and the supernatant was incubated overnight with primary antibody (Anti-FLAG; 1:1000; F3165 Sigma). The next morning, the samples were incubated with Protein G Sepharose for 2 h to capture the FLAG-MELK/FLAG-MELK$^{1\text{-}340}$. The beads were then washed with lysis buffer (20 mM Tris-HCl pH 7.5, 150 mM NaCl, 1% NP-40, 0.5% sodium deoxycholate). Finally, the samples were eluted with 100 μL SDS sample buffer. Both cell lysates and co-immunoprecipitated samples were subjected to Western blotting using antibodies against arrestin (1:10,000; polyclonal rabbit F431 [58]) and MELK (1:1000; F3165 Sigma).

4.7. Cellular proliferation assay

HEK293 arrestin-2/3 knockout cells were either left untransfected or transfected with HA-arrestin-3 (1 μg), FLAG-MELK$^{1\text{-}340}$ (1 μg), or a fixed ratio of the two plasmids for 46 h prior to treatment with 10 mM EdU (5-ethynyl-2′-deoxyuridine) for 2 h. Cells were then detached from support using 0.025% trypsin, and the protease was quenched with DMEM medium (10% FBS, 1% Pen/Strep). Cells were immediately washed with 3 mL of 1% bovine serum albumin (BSA) in PBS and centrifuged at 700 ×*g*. The pellet was then fixed for 15 min at room temperature with 4% paraformaldehyde in PBS and the wash step was repeated. A 100 μL saponin-based permeabilization and wash reagent was used to prepare the cells for the Click-iT™ reaction (ThermoFisher Scientific).

A Click-iT™ reaction mixture was prepared using PBS, copper protectant, reaction buffer additive, and picolyl azide fluorescent dye following manufacturer's instructions (ThermoFisher Scientific). Cells were incubated with 500 μL of the mixture for 30 min prior to a final wash with saponin-based permeabilization and wash reagent. Cells were resuspended in 500 μL buffer and analyzed using flow cytometry. Flow analysis was performed using a 3-laser LSRII (BD Biosciences). Analysis of flow cytometry data was performed using FlowJo 10.1.5 (FlowJo LLC, Ashland, OR).

4.8. Statistical analysis

Statistical methods used are indicated in figure legends.

Funding

This work was supported by American Heart Association 16PRE30180007 (NAP) and 18PRE34030017 (NAP), NIH grants R35 GM122491 (VVG), GM120569 (TMI), GM123252 (KND), DA043680 (TMI/VVG), Vanderbilt Discovery Award (TMI/VVG), Cancer Research and Prevention Institute of Texas (CPRIT) (RP160657) (KND), and the Welch Foundation (F-1390) (KND). The VMC Flow Cytometry Shared Resource is supported by the Vanderbilt Ingram Cancer Center (P30 CA68485) and the Vanderbilt Digestive Disease Research Center (DK058404).

Author contributions

NAP designed research; NAP, KPF, TSK, AIK and AC performed experiments; NAP and KPF analyzed data; JMT and KND contributed reagents/analytical tools; NAP wrote the paper with input from KND, TMI, and VVG. All authors approved the final version of the manuscript.

Declaration of Competing Interest

None.

Acknowledgements

The authors are grateful to Dr. Asuka Inoue for the generous gift of the arrestin-2/3 knockout HEK293 cells and Dr. Chad Brautigam for discussions of MST data analysis. The authors also thank Brittany Matlock for technical assistance with flow cytometry experiments, which were performed in the VMC Flow Cytometry Shared Resource.

Appendix A. Supplementary data

Supplementary data to this article can be found online at https://doi.org/10.1016/j.cellsig.2019.109366.

References

[1] R. Ganguly, A. Mohyeldin, J. Thiel, H.I. Kornblum, M. Beullens, I. Nakano, MELK—a conserved kinase: functions, signaling, cancer, and controversy, Clin. Transl. Med. 4 (2015) 11.
[2] J.M. Lizcano, O. Göransson, R. Toth, M. Deak, N.A. Morrice, J. Boudeau, et al., LKB1 is a master kinase that activates 13 kinases of the AMPK subfamily, including MARK/PAR-1, EMBO J. 23 (2004) 833–843.
[3] H. Jung, H.-A. Seong, H. Ha, Murine protein serine/threonine kinase 38 activates apoptosis signal-regulating kinase 1 via Thr838 phosphorylation, J. Biol. Chem. 283 (2008) 34541–34553.
[4] C.J. Giuliano, A. Lin, J.C. Smith, A.C. Palladino, J.M. Sheltzer, MELK expression correlates with tumor mitotic activity but is not required for cancer growth, eLife 7 (2018) e32838.
[5] C. Speers, S.G. Zhao, V. Kothari, A. Santola, M. Liu, K. Wilder-Romans, et al., Maternal embryonic leucine zipper kinase (MELK) as a novel mediator and biomarker of radioresistance in human breast cancer, Clin. Cancer Res. 22 (2016) 5864.
[6] K. Joshi, Y. Banasavadi-Siddegowda, X. Mo, S.H. Kim, P. Mao, C. Kig, et al., MELK-dependent FOXM1 phosphorylation is essential for proliferation of glioma stem cells, Stem Cells 31 (2013) 1051–1063.
[7] L. Beke, C. Kig, J.T.M. Linders, S. Boens, A. Boeckx, E. Van Heerde, et al., MELK-T1, a small-molecule inhibitor of protein kinase MELK, decreases DNA-damage tolerance in proliferating cancer cells, Biosci. Rep. 35 (6) (2015) e00267.
[8] Y. Wang, M. Begley, Q. Li, H.-T. Huang, A. Lako, M.J. Eck, et al., Mitotic MELK-eIF4B signaling controls protein synthesis and tumor cell survival, Proc. Natl. Acad. Sci. 113 (2016) 9810.
[9] M. Beullens, S. Vancauwenbergh, N. Morrice, R. Derua, H. Ceulemans, E. Waelkens, et al., Substrate specificity and activity regulation of protein kinase MELK, J. Biol. Chem. 280 (2005) 40003–40011.
[10] C. Gu, Y.K. Banasavadi-Siddegowda, K. Joshi, Y. Nakamura, H. Kurt, S. Gupta, et al., Tumor-specific activation of the C-JUN/MELK pathway regulates glioma stem cell growth in a p53-dependent manner, Stem Cells 31 (2013) 870–881.
[11] P. Jiang, D. Zhang, Maternal embryonic leucine zipper kinase (MELK): a novel regulator in cell cycle control, embryonic development, and cancer, Int. J. Mol. Sci. 14 (2013) 21551–21560.
[12] H.-A. Seong, R. Manoharan, H. Ha, Smad proteins differentially regulate obesity-induced glucose and lipid abnormalities and inflammation via class-specific control of AMPK-related kinase MPK38/MELK activity, Cell Death Dis. 9 (2018) 471.
[13] S.S.G. Ferguson, J. Zhang, L.S. Barak, M.G. Circ, Role of β-arrestins in the intraceliular trafficking of G-protein-coupled receptors, in: D.S. Goldstein, G. Eisenhofer, R. McCarty (Eds.), Advances in Pharmacology, Academic Press, 1997, pp. 420–424.
[14] S.S. Ferguson, Evolving concepts in G protein-coupled receptor endocytosis: the role in receptor desensitization and signaling, Pharmacol. Rev. 53 (2001) 1–24.
[15] O.B. Goodman, J.G. Krupnick, F. Santini, V.V. Gurevich, R.B. Penn, A.W. Gagnon, et al., Beta-arrestin acts as a clathrin adaptor in endocytosis of the beta2-adrenergic receptor, Nature 383 (1996) 447–450.
[16] O.B. Goodman, J.G. Krupnick, V.V. Gurevich, J.L. Benovic, J.H. Keen, Arrestin/clathrin interaction. Localization of the arrestin binding locus to the clathrin terminal domain, J. Biol. Chem. 272 (1997) 15017–15022.
[17] L.M. Luttrell, S.S. Ferguson, Y. Daaka, W.E. Miller, S. Maudsley, G.J. Della Rocca, et al., Beta-arrestin-dependent formation of beta2 adrenergic receptor-Src protein kinase complexes, Science 283 (1999) 655–661.
[18] J. Barlic, J.D. Andrews, A.A. Kelvin, S.E. Bosinger, M.E. DeVries, L. Xu, et al., Regulation of tyrosine kinase activation and granule release through β-arrestin by CXCR1, Nat. Immunol. 1 (2000) 227.
[19] M. Breitman, S. Kook, L.E. Gimenez, B.N. Lizama, M.C. Palazzo, E.V. Gurevich, et al., Silent scaffolds: inhibition of c-Jun N-terminal kinase 3 activity in cell by dominant-negative arrestin-3 mutant, J. Biol. Chem. 287 (2012) 19653–19664.
[20] M.D. Brown, D.B. Sacks, Protein scaffolds in MAP kinase signalling, Cell. Signal. 21 (2009) 462–469.
[21] S. Kook, X. Zhan, T.S. Kaoud, K.N. Dalby, V.V. Gurevich, E.V. Gurevich, Arrestin-3 binds c-Jun N-terminal kinase 1 (JNK1) and JNK2 and facilitates the activation of these ubiquitous JNK isoforms in cells via scaffolding, J. Biol. Chem. 288 (2013) 37332–37342.
[22] P.H. McDonald, C.W. Chow, W.E. Miller, S.A. Laporte, M.E. Field, F.T. Lin, et al., Beta-arrestin 2: a receptor-regulated MAPK scaffold for the activation of JNK3,

Science 290 (2000) 1574–1577.
[23] X. Zhan, T.S. Kaoud, S. Kook, K.N. Dalby, V.V. Gurevich, JNK3 enzyme binding to arrestin-3 differentially affects the recruitment of upstream mitogen-activated protein (MAP) kinase kinases, J. Biol. Chem. 288 (2013) 28535–28547.
[24] M.R. Ahmed, X. Zhan, X. Song, S. Kook, V.V. Gurevich, E.V. Gurevich, Ubiquitin ligase parkin promotes Mdm2–arrestin interaction but inhibits arrestin ubiquitination, Biochemistry. 50 (2011) 3749–3763.
[25] L. Girnita, S.K. Shenoy, B. Sehat, R. Vasilcanu, A. Girnita, R.J. Lefkowitz, et al., β-Arrestin is crucial for ubiquitination and down-regulation of the insulin-like growth Factor-1 receptor by acting as adaptor for the MDM2 E3 ligase, J. Biol. Chem. 280 (2005) 24412–24419.
[26] K. Xiao, D.B. McClatchy, A.K. Shukla, Y. Zhao, M. Chen, S.K. Shenoy, et al., Functional specialization of β-arrestin interactions revealed by proteomic analysis, Proc. Natl. Acad. Sci. 104 (2007) 12011–12016.
[27] N.A. Perry, T.S. Kaoud, O.O. Ortega, A.I. Kaya, D.J. Marcus, J.M. Pleinis, et al., Arrestin-3 scaffolding of the JNK3 cascade suggests a mechanism for signal amplification, Proc. Natl. Acad. Sci. (2018) 201819230.
[28] S. Coffa, M. Breitman, S.M. Hanson, K. Callaway, S. Kook, K.N. Dalby, et al., The effect of arrestin conformation on the recruitment of c-Raf1, MEK1, and ERK1/2 activation, PLoS One 6 (2011) e28723.
[29] L.M. Luttrell, W.E. Miller, Chapter five - arrestins as regulators of kinases and phosphatases, in: L.M. Luttrell (Ed.), Progress in Molecular Biology and Translational Science, Academic Press, 2013, pp. 115–147.
[30] C. Guo, A.J. Whitmarsh, The beta-arrestin-2 scaffold protein promotes c-Jun N-terminal kinase-3 activation by binding to its nonconserved N terminus, J. Biol. Chem. 283 (2008) 15903–15911.
[31] X. Li, R. MacLeod, A.J. Dunlop, H.V. Edwards, N. Advant, L.C.D. Gibson, et al., A scanning peptide array approach uncovers association sites within the JNK/βarrestin signalling complex, FEBS Lett. 583 (2009) 3310–3316.
[32] Y.-S. Cho, J. Yoo, S. Park, H.-S. Cho, The structures of the kinase domain and UBA domain of MPK38 suggest the activation mechanism for kinase activity, Acta Crystallogr. D Biol. Crystallogr. 70 (2014) 514–521.
[33] Q. Chen, N.A. Perry, S.A. Vishnivetskiy, S. Berndt, N.C. Gilbert, Y. Zhuo, et al., Structural basis of arrestin-3 activation and signaling, Nat. Commun. 8 (2017) 1427.
[34] W.E. Miller, R.J. Lefkowitz, Expanding roles for β-arrestins as scaffolds and adapters in GPCR signaling and trafficking, Curr. Opin. Cell Biol. 13 (2001) 139–145.
[35] X. Zhan, A. Perez, L.E. Gimenez, S.A. Vishnivetskiy, V.V. Gurevich, Arrestin-3 binds the MAP kinase JNK3a2 via multiple sites on both domains, Cell. Signal. 26 (2014) 766–776.
[36] N.A. Perry, X. Zhan, E.V. Gurevich, T.M. Iverson, V.V. Gurevich, Using in vitro pull-down and in-cell overexpression assays to study protein interactions with arrestin, in: M.G.H. Scott, S.A. Laporte (Eds.), Beta-Arrestins: Methods and Protocols, Springer New York, New York, NY, 2019, pp. 107–120.
[37] M. Jerabek-Willemsen, C.J. Wienken, D. Braun, P. Baaske, S. Duhr, Molecular interaction studies using microscale thermophoresis, Assay Drug Dev. Technol. 9 (2011) 342–353.
[38] H. Amartely, A. Iosub-Amir, A. Friedler, Identifying protein-protein interaction sites using peptide arrays, J. Visual. Exp. 52097 (2014).
[39] C. Katz, L. Levy-Beladev, S. Rotem-Bamberger, T. Rito, S.G.D. Rüdiger, A. Friedler, Studying protein–protein interactions using peptide arrays, Chem. Soc. Rev. 40 (2011) 2131–2145.
[40] X. Zhan, L.E. Gimenez, V.V. Gurevich, B.W. Spiller, Crystal structure of arrestin-3 reveals the basis of the difference in receptor binding between two non-visual arrestins, J. Mol. Biol. 406 (2011) 467–478.
[41] X. Song, S. Coffa, H. Fu, V.V. Gurevich, How does arrestin assemble MAPKs into a signaling complex? J. Biol. Chem. 284 (2009) 685–695.
[42] L.S. Cao, J. Wang, Y. Chen, H. Deng, Z.X. Wang, J.W. Wu, Structural basis for the regulation of maternal embryonic leucine zipper kinase, PLoS One 8 (2013) e70031.
[43] K. Moravcevic, J.M. Mendrola, K.R. Schmitz, Y.-H. Wang, D. Slochower, P.A. Janmey, et al., Kinase associated-1 domains drive MARK/PAR1 kinases to membrane targets by binding acidic phospholipids, Cell. 143 (2010) 966–977.
[44] B. Nolen, S. Taylor, G. Ghosh, Regulation of protein kinases: controlling activity through activation segment conformation, Mol. Cell 15 (2004) 661–675.
[45] G. Canevari, S. Re Depaolini, U. Cucchi, J.A. Bertrand, E. Casale, C. Perrera, et al., Structural insight into maternal embryonic leucine zipper kinase (MELK) conformation and inhibition toward structure-based drug design, Biochemistry. 52 (2013) 6380–6387.
[46] C.N. Johnson, V. Berdini, L. Beke, P. Bonnet, D. Brehmer, J.E. Coyle, et al., Fragment-based discovery of type I inhibitors of maternal embryonic leucine zipper kinase, ACS Med. Chem. Lett. 6 (2015) 25–30.
[47] B.B. Touré, J. Giraldes, T. Smith, E.R. Sprague, Y. Wang, S. Mathieu, et al., Toward the validation of maternal embryonic leucine zipper kinase: discovery, optimization of highly potent and selective inhibitors, and preliminary biology insight, J. Med. Chem. 59 (2016) 4711–4723.
[48] S. Klaeger, S. Heinzlmeir, M. Wilhelm, H. Polzer, B. Vick, P.-A. Koenig, et al., The target landscape of clinical kinase drugs, Science 358 (2017).
[49] A. Salic, T.J. Mitchison, A chemical method for fast and sensitive detection of DNA synthesis in vivo, Proc. Natl. Acad. Sci. 105 (2008) 2415.
[50] M. Grundmann, N. Merten, D. Malfacini, A. Inoue, P. Preis, K. Simon, et al., Lack of beta-arrestin signaling in the absence of active G proteins, Nat. Commun. 9 (2018) 341.
[51] J. Seo, E.L. Tsakem, M. Breitman, V.V. Gurevich, Identification of arrestin-3-specific residues necessary for JNK3 activation, J. Biol. Chem. 286 (2011) 27894–27901.
[52] X. Zhan, H. Stoy, T.S. Kaoud, N.A. Perry, Q. Chen, A. Perez, et al., Peptide mini-scaffold facilitates JNK3 activation in cells, Sci. Rep. 6 (2016) 21025.
[53] S.M. Hanson, W.M. Cleghorn, D.J. Francis, S.A. Vishnivetskiy, D. Raman, X. Song, K.S. Nair, V.Z. Slepak, C.S. Klug, V.V. Gurevich, Arrestin mobilizes signaling proteins to the cytoskeleton and redirects their activity, J. Mol. Biol. 368 (2007) 375–387.
[54] S.K. Shenoy, P.H. McDonald, T.A. Kohout, R.J. Lefkowitz, Regulation of receptor fate by ubiquitination of activated beta 2-adrenergic receptor and beta-arrestin, Science 294 (2001) 1307–1313.
[55] I. Chartrain, Y. Le Page, G. Hatte, R. Körner, J.Z. Kubiak, J.-P. Tassan, Cell-cycle dependent localization of MELK and its new partner RACK1 in epithelial versus mesenchyme-like cells in Xenopus embryo, Biol. Open 2 (2013) 1037–1048.
[56] N. Tochio, S. Koshiba, N. Kobayashi, M. Inoue, T. Yabuki, M. Aoki, et al., Solution structure of the kinase-associated domain 1 of mouse microtubule-associated protein/microtubule affinity-regulating kinase 3, Protein Sci. 15 (2006) 2534–2543.
[57] X. Zhan, T.S. Kaoud, K.N. Dalby, V.V. Gurevich, Non-visual arrestins function as simple scaffolds assembling the MKK4–JNK3a2 signaling complex, Biochemistry 50 (2011) 10520–10529.
[58] S.A. Vishnivetskiy, X. Zhan, Q. Chen, T.M. Iverson, V.V. Gurevich, et al., Curr. Protoc. Pharmacol. 67 (2014) Unit 2.11.1-9.
[59] S.C. Tso, Q. Chen, S.A. Vishnivetskiy, V.V. Gurevich, T.M. Iverson, C.A. Brutigam, Using two-site binding models to analyze microscale thermophoresis data, Anal. Biochem. 540-541 (2017) 64–75.
[60] T.H. Scheuermann, S.B. Padrick, K.H. Gardner, C.A. Brautigam, On the acquisition and analysis of microscale thermophoresis data, Anal. Biochem. 496 (2016) 79–93.
[61] Y.Y. Yim, K. Betke, H. Hamm, Using peptide arrays created by the SPOT method for defining protein-protein interactions, in: C.L. Meyerkord, H. Fu (Eds.), Protein-Protein Interactions: Methods and Applications, Springer New York, New York, NY, 2015, pp. 307–320.
[62] E. Alvarez-Curto, A. Inoue, L. Jenkins, S.Z. Raihan, R. Prihandoko, A.B. Tobin, et al., Targeted elimination of G proteins and Arrestins defines their specific contributions to both intensity and duration of G protein-coupled receptor signaling, J. Biol. Chem. 291 (2016) 27147–27159.